Energy dependent wavelength of the ion induced nanoscale ripple

T. K. Chini,* M. K. Sanyal, and S. R. Bhattacharyya
Surface Physics Division, Saha Institute of Nuclear Physics, 1/AF Bidhannagar, Kolkata 700 064, India

Wavelength variation of ion beam induced nanoscale ripple structure has received much attention recently due to its possible application in nanotechnology. We present here results of Ar^+ bombarded Si in the energy range 50 to 140 keV to demonstrate that with beam scanning the ripple wavelength increases with ion energy and decreases with energy for irradiation without ion beam scanning. An expression for the energy dependence of ripple wavelength is proposed taking into simultaneous effect of thermally activated surface diffusion and ion induced effective surface diffusion.

PACS numbers: 68.35.Bs, 79.20.Rf, 64.60.Ht

Formation of periodic undulations or ripple like features on various materials with typical wavelength ranging from about 10 nm to 1μm, obtained by obliquely incident ion bombardment, has become an active research subject due to its possible technological applications, as varied as optical devices, templates for liquid crystal orientation and strain-free patterned substrates for heteroepitaxial growth of quantum wires. It is also expected that systematic study of ion beam induced nano ripple formation will help us to understand the basic processes prevalent in formation of sand dune like structures in deserts. Although this ion induced phenomenon was reported first in 1960s [1] and then in 1970s [2, 3], the improvement in experimental conditions such as, better vacuum and ion beam parameters and improved surface characterizing tools, has enabled us to control the growth of these ripple like features [4, 5, 6, 7, 8, 9, 10, 11]. The first widely accepted theoretical approach describing the process of ripple formation due to ion bombardment was developed by Bradley and Harper (BH) [12]. This linear theory [12] predicts the ripple wavelength and orientation in agreement with numerous experimental studies. However, this theory cannot explain a number of experimental observations, such as the saturation of the ripple amplitude [9], the appearance of rotated ripples [11] and kinetic roughening [13]. Moreover, according to the BH theory ripple wavelength should decrease with ion energy but this prediction has not been confirmed experimentally so far [5, 6, 7].

Recently a formalism [14, 15, 16] based on nonlinear continuum theory has been developed to understand these experimental observations not predicted by linear theory. In this new formalism, not only nonlinear and noise terms were included in the equation of height profile for eroded surface but also existence of two different surface diffusion processes were recognised. Based on Sigmund's theory of sputtering [17], the height evolution $h(x, y, t)$ of an ion eroded surface according to this nonlinear theory [14, 15, 16] can be described by

$$\partial_t h = \nu\nabla^2 h - (D^T + D^I)\nabla^4 h + \frac{\lambda}{2}(\nabla h)^2 + \eta(x, y, t). \quad (1)$$

Here ν is the roughening prefactor (also called effective surface tension), generated by the ion bombardment sputter-erosion process. D^T & D^I are designated as thermally activated surface diffusion constant and ion induced effective surface diffusion (ESD) constant. The nonlinear term λ represent the slope dependent erosion rate, where (∇h) define the local slopes and $\eta(x, y, t)$ is an uncorrelated white noise with zero average, mimicking the local random fluctuation of the incident ion flux. All the coefficients of Eq. (1) can be made directional in (x, y) space and their detailed expressions are known [14, 16]. It is interesting to note that beyond a cross-over time, $\tau \sim (D/\nu^2)\ln(\nu/\lambda)$, the nonlinear terms become dominating and this effect is expected to generate many novel phenomena like ripple rotation in oblique ion incidence [11] and formation of dots and holes for normally incident ion beams [16]. On the otherhand for time, $t \ll \tau$, nonlinear and noise terms can be neglected $(\lambda = 0, \eta = 0)$ and Eq. 1 reduces to the BH theory [12] except for the fact that surface diffusion constant K has two components $K = D^I + D^T$. In the linear regime the balance of the unstable negative sputter-erosion term $(-|\nu|\partial^2 h)$, trying to roughen the surface and the positive surface diffusion term $(K\nabla^4 h)$ acting to smooth the surface, gives rise to observable ripple with wavelength

$$l_i = 2\pi\sqrt{2K/|\nu_i|}, \quad (2)$$

where, i refers to the direction x or y along which the associated $|\nu_i|$ ($|\nu_x|$ or $|\nu_y|$) is largest.

The ion induced ESD process predicts increase of ripple wavelength (l) with ion energy (E) but the thermal diffusion process, assumed to be dominating at high temperature, predicts reduction of l with increasing E. While the increase of l with E has been observed experimentally [6, 7, 18], direct observation of decreasing l with increasing E has not been reported so far to the best of our knowledge, even when the sample temperature is varied [5]. We have performed Ar^+ bombardment on Si(001) in 50-140 keV energy region and kept the bombardment process well within the linear region to verify experimentally the existence of these two diffusion processes and to understand the interplay between them in determining the wavelength of nanoscale ripple structure.

The ion bombardment of Si targets (p type Si(001) single crystal wafer) was undertaken with a high current ion accelerator (Danfysik) which is described in detail elsewhere [19]. These Si samples were irradiated in the implantation chamber (having a base vacuum in the range of 10^{-7} mbar) by a focused (with typical beam spot size of 1.5 mm and 2.5 mm) $^{40}Ar^{+}$ beam at 60^{o} angle of ion incidence with respect to surface normal of the samples. With a magnetic $x-y$ sweeping system the focused beam was scanned over the sample to maintain homogeneous irradiation. The scanned area could be varied from 5 mm $\times$ 5 mm to 15 mm $\times$ 15 mm. To check the influence of the beam scanning, several samples were irradiated without beam scanning. The beam flux in the present experiment was around 140 μA/cm^2 for irradiation without beam scanning. As the area of the bombarded spot on the sample for unscanned focused beam was smaller than that for the case of scanned beam, the period of bombardment was adjusted to give same dose of 10^{18} ions/cm^2 for all the irradiated samples. The maximum period of bombardment in the present case was always less than 1 hr, which is far less than the estimated cross-over time τ (about 3 hrs for 50 keV and 4 hrs for 100 keV) [15] ensuring the present experimental condition to be well within the linear regime. Thus, a higher dose of (3-4)$\times 10^{18}$ ions/cm^2 is required to expect any nonlinear effect whose signature has indeed been observed in our preliminary results reported elsewhere [20] for the case of morphology developed on GaAs bombarded by 60 keV Ar beam.

After irradiation, the samples were investigated by atomic force microscopy (AFM) in contact mode under ambient condition as described earlier [19, 20, 21]. Fig. 1 shows representative AFM images of Si(001) samples bombarded at 50 and 100 keV with and without beam scanning. Ripple topographies are clearly visible in all the AFM micrographs and they are oriented perpendicular to the ion-beam projection (indicated by arrowmarks) onto the surface as predicted by linear theory. The ripples grew uniformly on the whole bombarded spot for irradiation with beam scanning whereas ripples were developed at the central region of the bombarded spot for irradiation without scanning. The mean amplitude of the ripples with and without beam scanning, obtained from AFM measurements, are also shown in fig. 1. The most probable observed wavelength (l) of ripples, obtained from AFM images and Fourier analysis is given in fig. 2. With beam scanning l grows from about 700 nm to about 1000 nm as the incident ion energy (E) increases from 50 keV to 140 keV. However, the l decays from 600 nm to about 400 nm with the increasing E when the ripple is formed without beam scanning. If thermally activated surface diffusion is the dominant process for surface smoothing, the wavelength dependence on energy (E) of bombardment is given by [12] $l \sim E^{-1/2}$. On the otherhand in the absence of thermal diffusion, ion-induced ESD becomes dominating contributor in K and we expect [14] the energy dependence as $l \sim E$. The variation of l with E of the present experiment has exhibited both the trends : one increasing and other decreasing with the energy giving rise to exponents of 0.45 and -0.56 respectively (refer Fig. 2).

When the sample is bombarded with a focused beam without scanning, the beam intensity at the center of the bombarded spot becomes more than its peripheral region causing a local temperature rise. As the semiconductor sample in the present case is clamped on a copper block, good thermal contact is not ensured favouring the local temperature rise due to ion beam heating. Under this situation, the rise of temperature, T, from the initial ambient temperature , $T_o = 25^{o}C$, at time t(sec) of the commencement of the bombardment can be calculated from the formula [22]

$$t = \int_{T_o}^{T} \frac{S\kappa\rho}{P - (T^4 - T_o^4)} dT, \qquad (3)$$

where S,κ and ρ are specific heat (0.836 $J/g/^{o}C$), thickness (0.47 mm) and density (2.32 g/cm^3) respectively of the Si wafer used in the present experiment. Sample temperature thus estimated within 68 sec [22] after the start of bombardment was $\sim 800^{o}C$ for a beam power, P = 14 watt/cm^2 corresponding to the maximum flux (140μA/cm^2) employed in the present case for bombardment at 100 keV. As the period of bombardment is much higher than this rise time, beam induced heating is expected to be appreciable in the present case for the bombardment without scanning. Thus, thermally activated surface diffusion plays an important role here giving rise to a negative exponent $l \sim E^{-0.56}$, as expected from linear theory. It seems, the surface temperature profile on the sample generated by unscanned focused ion beam has made thermally activated diffusion process the dominating one. This was not the case even when experiments were performed by increasing the bulk temperature of the sample [5]. It should be mentioned here that we did not observe any flux dependence of the measured l in the flux range of 15 to 140 μA/cm^2 used here as predicted in BH model.

On the otherhand, for irradiation with beam scanning, effective beam intensity on the bombarded spot is reduced as the beam is sweeped continuously over the sample. The magnetic beam sweeping system of our implanter uses scan frequencies of 0.51 Hz and 5.3 Hz along the horizontal and vertical direction to maintain beam homogeneity on the irradiated area of the sample. This means, each region of the bombarded spot of the size of beam diameter will be exposed to the ion beam every after few seconds only which is much less than the time of rise of the maximum equilibrium temperature due to beam heating. So promotion of surface diffusion of thermal origin will be hampered and ion induced surface diffusion will be the main relaxation process in the case

of beam scanning. However, at relatively lower energy thermal contribution may become noticeable.

We can rewrite the ripple wavelength expressed by Eq. 2 by splitting the two diffusion terms as

$$l^2 = 8\pi^2 \frac{D^T + D^I}{|\nu|} \tag{4}$$

which can be approximated as

$$l^2 = A + BE^{-1} + CE^2 \tag{5}$$

where A, B and C are fitting parameters. In this approximation, we have assumed that both depth (a) and longitudinal spread (α) are linear with energy, as obtained exponents from TRIM calculations [23] are close to unity (refer Fig. 2). It is possible to determine the shape of the distribution of the deposited energy density in the near surface region induced by the ion collision cascades. As for example, for the case of ripple topography formation on Ar bombarded graphite in 2 -50 keV energy region Habenicht *et al* [7] obtained a power law relation $l(E) \sim E^p$ ($p = 0.95$) while a and α scale with ion energy implying an energy-independent lateral spread of the damage cascade. However, we obtained $l(E) \sim E^p$ ($p = 0.45$) with beam scanning (Fig. 2). A lower exponent ($p \ll 1$) is an indication of the changing lateral spread of the damage cascade with the ion energy for the energy region selected in the present experimental situation. The modified expression (Eq. 5) of the energy dependence of ripple wavelength now considers the simultaneous effect of ion induced effective surface diffusion and thermally activated surface diffusion.

The growth and decay of l with E of the present experimental results (Fig. 3a) can be fitted with Eq. 5 with fitting parameters $A = 311697$, $B = 2.5 \times 10^6$ and $C = 41.5$ for the ripple formation with beam scanning. The corresponding values for the ripple wavelength without beam scanning is $A = -195533$, $B = 2.9 \times 10^7$ and $C = 8.0$. Here l and E are expressed in nm and keV respectively. The higher value of the coefficient of the second term for fitting the ripple wavelength data without beam scanning signifies that contribution of thermally activated surface diffusion is higher than that prevalent with beam scanning.

To test the validity of our proposed formalism we have also used it for the data of Flamm *et al* [18] where ripple structures with a characteristic wavelength between 30 and 300 nm are formed on fused silica at room temperature after irradiation by broad beam ion (Ar) source in the energy region 0.6 to 1.5 keV. The expected dominance of ion induced effective surface diffusion has been reflected in this case by the excellent fit of the data (Fig. 3b) with Eq. 5 having much higher value of the coefficient of the ion induced diffusion term ($C = 19861$) over the value of the coefficient ($B = 6077.8$) representing the thermal diffusion term. Thus, our proposed formula behaves consistently with homogeneous bombardment condition from the low ($\sim$ 1 keV) to the medium ($\sim$ few hundreds keV) energy regime where the concept of linear collision cascade model holds for heavy ion bombardment on solid target.

In summary, we have experimentally verified, for the first time, the existence and interplay of two types of diffusion mechanism prevalent in ion induced nanoscale nanoscale ripple formation giving rise to the increasing or decreasing tendency of the ripple wavelength with ion energy. We have proposed a formalism for the ripple wavelength variation with the ion energy and verified its applicability over a wide energy range. The proposed formalism indicates that both thermal and ion induced surface diffusion act simultaneously to form stable ripple morphology. Ion beam induced surface temperature profile, rather than bulk temperature of the sample, seems to initiate the thermally activated diffusion process. It will be interesting to investigate the role of this temperature profile in the formation of uniform nanoscale ripple structure and in the nonlinear phenomena.

We would like to thank Mr. S. Roy and Mr. A. Das for their technical assistance and Dr. S. Hazra for valuable discussions.

* Electronic address: tapashp@hp2.saha.ernet.in

[1] M. Navez, S. Sella and D. Chaperot, Le Bombardement Ionique, CNRS, Bellevue, Paris (1962) p.233
[2] R. S. Nelson and D. J. Mazey, *Ion Surface Interactions, Sputtering and Related Phenomena*, (Gordon and Breach Ltd., London, 1973), p. 199.
[3] G. Carter, M. J. Nobes, F. Paton, J. S. Williams and J. L. Whiton, Rad. Effect. **33**, 65 (1977).
[4] J. Erlebacher, M. J. Aziz, E. Chason, M. B. Sinclair, J. A. Floro, Phys. Rev. Lett. **82**, 2330 (1999).
[5] G. Carter, V. Vishnyakov, Phys. Rev. B **54**, 17647 (1996).
[6] A. Datta, Y. R. Wu, Y. L. Wang, Phys. Rev. B **63**, 125407 (2001).
[7] S. Habenicht, W. Bolse, H. Feldermann, U. Geyer, H. Hofsäss, K. P. Lieb, F. Roccaforte, Europhys. Lett. **50**, 209 (2000).
[8] E. Chason *et al.*, Phys. Rev. Lett. **72**, 3040 (1994); T. M. Mayer *et al.*, J. Appl. Phys. **76**, 1633 (1994).
[9] J. Erlebacher, M. J. Aziz, E. Chason, M. B. Sinclair and J. A. Floro, J. Vac. Sci. Technol. **A 18**, 115 (2000).
[10] S. Facsko, T. Dekorsy, C. Koerdt, C. Trappe, H. Kurz, A. Vogt, and H. L. Hartnagel, Science **285**, 1551 (1999);
[11] S. Rusponi, G. Costantini, C. Boragno, and U. Valbusa, Phys. Rev. Lett. **81** 2735 (1998); S. Rusponi, G. Costantini, F. B. de Mongeot, C. Boragno, and U. Valbusa, Appl. Phys. Lett. **75**, 3318 (1999).
[12] R. M. Bradley, J. M. E Harper, J. Vac.Sci. Technol. A **6**, 2390 (1988).
[13] E. A. Eklund *et al.*, Phys. Rev. Lett. **67**, 1759 (1991); H. N. Yang *et al.*, Phys. Rev. **B 50**, 7635 (1994).
[14] R. Cuerno and A. L. Barabási, Phys. Rev. Lett. **74**,

4746 (1995); R. Cuerno *et al.*, Phys. Rev. Lett. **75**, 4464 (1995). M. A. Makeev, R. Cuerno, and A.-L. Barabási, http://xxx.lanl.gov/abs/cond-mat/0007354 (24 July 2000); M. A. Makeev and A.-L. Barabási, Appl. Phys. Lett. **71**, 2800 (1997).

[15] S. Park, B. Kahng, H. Jeong and A.-L. Barabási, Phys. Rev. Lett. **83**, 3486 (1999).

[16] B. Kahng, H. Jeong and A.-L. Barabási, Appl. Phys. Lett. **78**, 805 (2001).

[17] P. Sigmund, Phys. Rev. **184**, 383 (1969).

[18] D. Flamm, F. Frost and D. Hirsch, Appl. Surf. Sci. **179**, 95 (2001).

[19] T. K. Chini, D. Datta, S. R. Bhattacharyya, M. K. Sanyal, Appl. Surf. Sci. **182**, 313 (2001).

[20] D. Datta, T. K. Chini, S. R. Bhattacharyya and M. K. Sanyal, Proc. 19 th Intl. Conf. on Atomic Collisions in Solids, Paris (29 July-3 August, 2001)- to be published in Nucl. Instrum. Meth B (2002).

[21] J. K. Basu, S. Hazra and M. K. Sanyal, Phys. Rev. Lett., **82**, 4675 (1999).

[22] G. Dearnaley, J. H. Freeman, R. S. Nelson and J. Stephen, *Ion Implantation* (North-Holland Publishing Company, Amsterdam, 1973) p.423.

[23] J. F. Ziegler, J. P. Biersack, and U. Littmark, *The Stopping and Range of Ions in Solids* (Pergamon Press, New York, 1985). Also available from the web site www.srim.org.

FIG. 1: AFM micrographs of $^{40}Ar^{+}$ bombarded Si surfaces at two representative energy, namely, 50 keV and 100 keV : (a) and (b) with ion beam scanning; (c) and (d) without beam scanning. Arrow marks indicate the projection of ion beam onto the surface. Variation of mean amplitude of the ripples with ion energy is shown in the lower plot.

FIG. 2: Left scale depicts the variation of the mesaured wavelengths l as a function of the $^{40}Ar^{+}$ energy and the right scale shows the TRIM calculations for depth a and longitudinal straggling α as a function of ion energy. Power law fits to the wavelengths and TRIM data are inserted to each plot. The error bar of the measured data points have been determined after several repeated experiments and each data point represents the averages over different regions of the bombarded spot.

FIG. 3: (a) The square of the measured ripple wavelengths of the present experiment are fitted with Eq. (4). The function with the fitted parameters for the ripple wavelength data obtained with and without beam scanning are inserted within the graph. (b) The fitting of the data extracted from the measurements of Flamm *et al* [18]

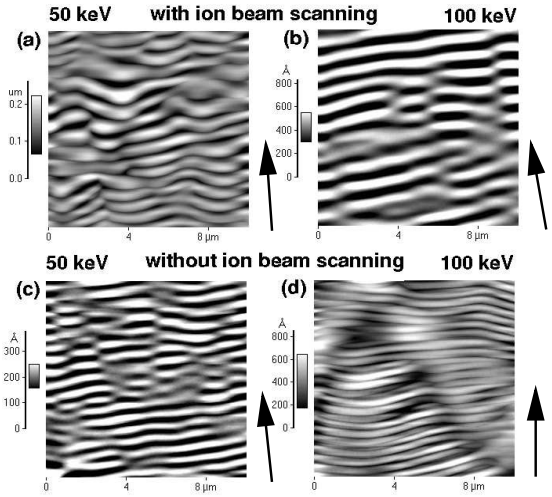
50 keV
with ion beam scanning
100 keV
(a)
(b)
50 keV
without ion beam scanning
100 keV
(c)
(d)

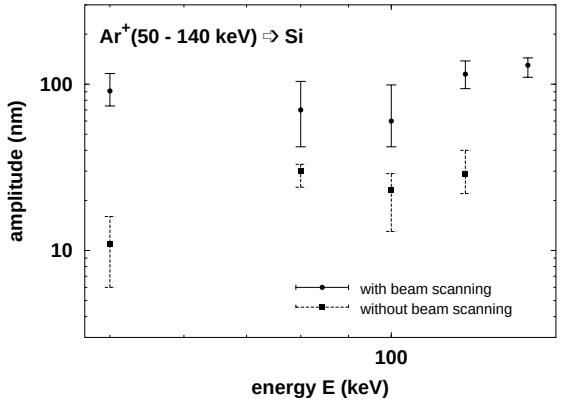
Ar+(50 - 140 keV) ⇨ Si
amplitude (nm)
100
10
with beam scanning
without beam scanning
100
energy E (keV)

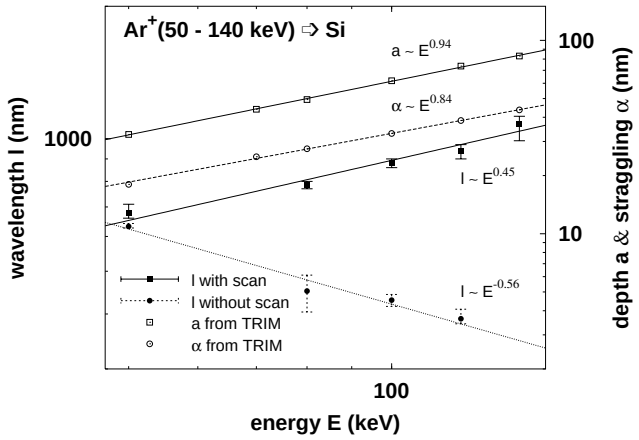
Ar+(50 - 140 keV) ⇨ Si
a ~ E0.94
α ~ E0.84
l ~ E0.45
l ~ E−0.56
l with scan
l without scan
a from TRIM
α from TRIM
wavelength l (nm)
1000
100
depth a & straggling α (nm)
100
10
energy E (keV)

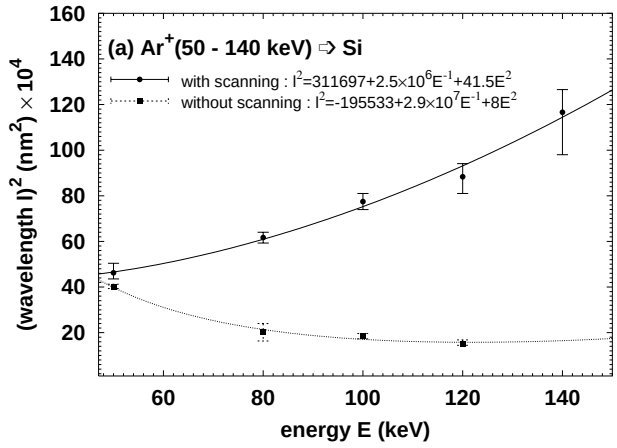
(a) Ar+(50 - 140 keV) ⇨ Si
with scanning : I2=311697+2.5×10^6E^-1+41.5E^2
without scanning : I2=-195533+2.9×10^7E^-1+8E^2
(wavelength l)2 (nm2) × 10^4
energy E (keV)
160
140
120
100
80
60
40
20
60
80
100
120
140

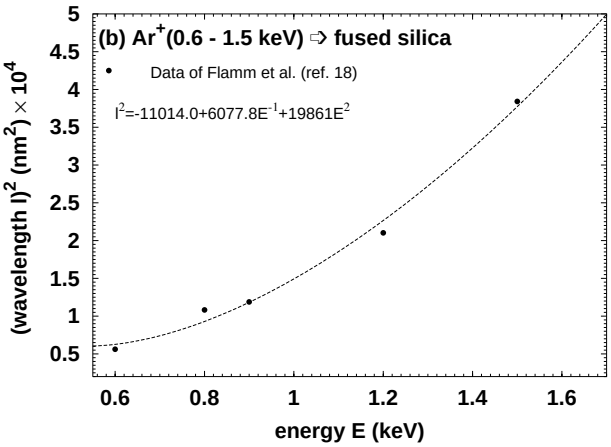
(b) Ar+(0.6 - 1.5 keV) ⇨ fused silica
Data of Flamm et al. (ref. 18)
I2=-11014.0+6077.8E^-1+19861E^2
(wavelength l)2 (nm2) × 10^4
energy E (keV)
5
4.5
4
3.5
3
2.5
2
1.5
1
0.5
0.6
0.8
1
1.2
1.4
1.6